ISSN 2472-1972

A Mitochondrial Progesterone Receptor Increases Cardiac Beta-Oxidation and Remodeling

Qunsheng Dai,[1] Creighton E. Likes, III,[1] Anthony L. Luz,[2] Lan Mao,[3] Jason S. Yeh,[1] Zhengzheng Wei,[4] Maragatha Kuchibhatla,[5] Olga R. Ilkayeva,[6] Timothy R. Koves,[6,7] and Thomas M. Price[1]

[1]Division of Reproductive Endocrinology, Duke University, Durham, North Carolina 27710; [2]Nicholas School of the Environment, Duke University, Durham, North Carolina 27710; [3]Division of Cardiology, Duke University, Durham, North Carolina 27710; [4]Center for Genomic and Computational Biology, Duke University, Durham, North Carolina 27710; [5]Division of Biostatistics and Bioinformatics, Sarah W. Stedman Nutrition and Metabolism Center, Duke University, Durham, North Carolina 27710; [6]Duke Molecular Physiology Institute, Duke University, Durham, North Carolina 27710; and [7]Division of Geriatrics, Duke University, Durham, North Carolina 27710

ORCiD numbers: 0000-0002-9720-7416 (T. M. Price).

Progesterone is primarily a pregnancy-related hormone, produced in substantial quantities after ovulation and during gestation. Traditionally known to function via nuclear receptors for transcriptional regulation, there is also evidence of nonnuclear action. A previously identified mitochondrial progesterone receptor (PR-M) increases cellular respiration in cell models. In these studies, we demonstrated that expression of PR-M in rat H9c2 cardiomyocytes resulted in a ligand-dependent increase in oxidative cellular respiration and beta-oxidation. Cardiac expression in a TET-On transgenic mouse resulted in gene expression of myofibril proteins for remodeling and proteins involved in oxidative phosphorylation and fatty acid metabolism. In a model of increased afterload from constant transverse aortic constriction, mice expressing PR-M showed a ligand-dependent preservation of cardiac function. From these observations, we propose that PR-M is responsible for progesterone-induced increases in cellular energy production and cardiac remodeling to meet the physiological demands of pregnancy.

Freeform/Key Words: pregnancy, mitochondria, respiratory chain, progesterone, beta-oxidation

Pregnancy increases physiologic stress to the human heart and is associated with a 45% increase in blood volume, a 35% decrease in systemic vascular resistance, and a 50% increase in cardiac output. Cardiac output increases throughout pregnancy and in early pregnancy is mostly attributable to increases in stroke volume, whereas the increase in later pregnancy is primarily due to an elevated heart rate (HR) [1]. These hemodynamic changes accompany compensatory cardiac changes, including increased ventricular mass and left ventricular

Abbreviations: %FS, percent fractional shortening; Aldob, aldolase B; Ampd2, adenosine monophosphate deaminase 2; Ct, threshold cycle; cTAC, constant transverse aortic constriction; Dox, doxycycline; ECAR, extracellular acidification rate; ELCa, essential light chain atrium; ER, estrogen receptor; GSEA, gene set enrichment analysis; HBD, hormone-binding domain; HR, heart rate; IHC, immunohistochemical; LVDd, left ventricular end-diastolic dimension; LVDs, left ventricular end-systolic dimension; mGAPDH, mouse glyceraldehyde 3-phosphate dehydrogenase; mVcfc, mean velocity of circumferential shortening corrected by heart rate; Myl, myosin light polypeptide; neg, mice not expressing mitochondrial progesterone receptor; Nppb, natriuretic peptide type B; nPR, nuclear progesterone receptor; OCR, oxygen consumption rate; PCH, physiological cardiac hypertrophy; pos, mice expressing mitochondrial progesterone receptor; PR-M, mitochondrial progesterone receptor; rtTA, reverse tetracycline transactivator; SERCA, sarcoplasmic reticulum calcium ATPase; Sln, sarcolipin; SR, sarcoplasmic reticulum; TCA, tricarboxylic acid.

Received 3 August 2018
Accepted 28 December 2018
First Published Online 3 January 2019

end-diastolic volume, whereas end-systolic volume remains unchanged. This preserved cardiac ejection capability is primarily due to decreased systemic vascular resistance, resulting in decreased afterload. The cardiac changes in pregnancy are similar, but not identical, to those seen with endurance exercise training and referred to as physiological cardiac hypertrophy (PCH). Heart remodeling with PCH is associated with reversible myocyte hypertrophy and the formation of new sarcomeres [2]. Normally the cardiac changes of pregnancy return to normal after delivery, but long-term left ventricular hypertrophy with dysfunction may be seen in women with preeclampsia [3]. In more extreme circumstances, the condition progresses to greater dilatation with failure, termed peripartum cardiomyopathy [4].

The normal myocardium primarily relies on oxidative phosphorylation and, to a much lesser degree, glycolysis for ATP generation. Typically, substrates consist of 60% to 90% fatty acids and 10% to 40% glucose [5]. Substrates for energy production in the myocardium include fatty acids, amino acids, ketones, pyruvate, and carbohydrates [6]. Sex differences in myocardial metabolism are apparent. Compared with males, the reproductive-age female heart has greater fatty acid metabolism associated with increased energy yield and oxygen consumption. Thus, in situations with replete energy substrates, the reproductive-age female heart appears to have greater capacity than the male heart, but this capacity may be compromised in conditions of low oxygen supply [6].

Little is known of the mechanisms that enhance myocardial energy production to meet the increased metabolic demands of pregnancy. Although many biochemical changes are associated with pregnancy, the dramatic increase in the sex steroids estrogen and progesterone predominate. This report focuses on the role of a mitochondrial progesterone receptor (PR-M) in controlling myocardial energy production. PR-M is a truncated isoform of the nuclear PR (nPR). Unlike nPR, which contains protein domains of an N-terminal transcriptional activation domain, a DNA-binding domain, a hinge region, and a hormone-binding domain (HBD), PR-M is characterized by an N-terminus mitochondrial localization sequence followed by the hinge and HBD [7]. PR-M localizes to the mitochondrial outer membrane and functions to increase cellular respiration in a ligand-dependent mechanism [8]. The sequence for PR-M with the putative translation start site in the distal third intron of the PR gene is found in humans and nonhuman primates. The rodent genome shows no sequence similarity in the distal third intron. Thus, with only humans and nonhuman primates expressing this protein, *in vivo* manipulation with protein overexpression or knockdown is not feasible. Insight into the function of PR-M may be gained by overexpression in a rodent model. This report details the function of PR-M in modulating cellular energy production and remodeling in a transgenic mouse model and rat cardiac cell line.

1. Experimental Procedures

The experimental procedures are detailed in the supplemental data [9].

A. Rat H9c2 Cell Line

H9c2(2,1) [10] cells obtained from American Type Culture Collection (CRL-1446; Manassas, VA) were originally derived from embryonic BD1X rat heart tissue. Cells were maintained in DMEM (D-6429; Sigma) supplemented with 10% heat-inactivated fetal bovine serum at 37°C in a humidified atmosphere of 95% air and 5% CO_2. The cells were used between passages 19 and 28 in all experiments.

B. Transfection

H9c2 cells were cultured and grown in DMEM (D-6429) supplemented with 10% heat-inactivated fetal bovine serum growth media until 50% to 80% confluent then transfected with pEGFP-N1-PR-M plasmid with GeneJammer transfection reagent (Agilent Technologies,

Santa Clara, CA) according to the manufacturer's instructions. At 24 hours posttransfection, the cells were treated with synthetic progestin R5020 10^{-6} M or vehicle (alcohol) for 48 hours followed by gene expression analysis or fatty acid oxidation studies.

C. Fatty Acid Oxidation

Palmitic acid metabolism was determined by the release of tritiated water from [9,10-3H(N)]-palmitic acid (NET043001MC; PerkinElmer, Waltham, MA) with modifications of a previously described protocol [11]. Protein concentration was determined by Bio-Rad DC Protein Assay using the manufacturer's protocol (Bio-Rad, Hercules, CA).

D. Seahorse Extracellular Flux Analysis

Parameters of mitochondrial respiration [basal oxygen consumption rate (OCR), maximal OCR, spare respiratory capacity, proton leak, ATP-linked respiration, and extracellular acidification rate (ECAR)] were determined using the Seahorse XFe24 Extracellular Flux Analyzer (Seahorse Bioscience, North Billerica, MA). Prior to analysis, 25,000 cells were seeded into 24-well V7-PET plates (101037-004; Agilent Technologies), transfected with the PR-M or control vector, and treated with either R5020 or the vehicle for 24 hours. One hour before the assay, cell media was exchanged for assay media (DMEM supplemented with 25 mM glucose, 1 mM pyruvate, 4 mM glutamine, no bicarbonate, pH 7.4), and cells were incubated without CO_2 at 37°C for 1 hour. OCR was then measured under basal conditions, followed by the sequential injection of 1 μM oligomycin A (0.1% dimethyl sulfoxide), 1 μM carbonyl cyanide-4-(trifluoromethoxy)phenylhydrazone (0.1% dimethyl sulfoxide), 0.5 μM rotenone, and antimycin A (0.1% ethanol). Three basal OCR measurements were obtained prior to oligomycin injection, with an additional three OCR measurements after injection of each drug. Parameters were calculated per the manufacturer's instructions. Experiments were repeated at least three separate times.

E. Generation of PR-M Cassette

The entire open reading frame of PR-M [7] was PCR generated from a pPR-M/EGFP-N1 vector [8] with modifications including a Kozak sequence along with 5′ *Bam*H1 and 3′ Mlu1 restriction enzyme sites. The insert was ligated into pTRE-Tight (Clontech, Mountain View, CA) and propagated in One Shot® TOP10 Chemically Competent *E. coli* (Thermo Fisher Scientific, Austin, TX) by heat shock. The DNA cassette for oocyte injection was excised with *Xho*1 digestion, gel purified, and completely sequenced in both forward and reverse directions. Four base pair changes were noted from the original sequence, none of which resulted in an amino acid change (see supplemental data [9]).

F. Animals

All experimentation was approved by the Duke Institutional Animal Care and Use Committee, and animal care was provided by the Duke Laboratory of Animal Research. Tg(Myh6-rtTA)8585Jam mice (Myh6-rtTA) were obtained from Mutant Mouse Regional Resource Center at the University of Missouri (Columbia, MO). This transgenic mouse has a strain of FVB/J and is characterized by an α-cardiac myosin heavy chain promoter followed by a reverse tetracycline transactivator (rtTA), resulting in expression in cardiac myocytes.

PR-M–expressing mice were created by the Duke Transgenic Mouse Facility using DNA microinjection into embryos of the FVB/NHsd mouse strain (Harlan Laboratories, Houston, TX). Three founders were identified from 38 original progeny. Founders were initially bred with normal FVB mice, and subsequent F1 generations were bred with Myh6-rtTA mice. Of the original three founder lines, one was lost during breeding, and no experimental data were obtained, one yielded progeny that failed to show a cardiac PR-M transcript with doxycycline

(Dox) induction, and one yielded progeny showing induction of cardiac PR-M with Dox treatment (PR-M pos). Sperm were cryopreserved from the PR-M–positive mouse line.

The constant transverse aortic constriction (cTAC) studies, tissue injury histology, and metabolomics profiling were completed with mice from the original founder. Due to subsequent cessation of breeding, the line was rederived using previously cryopreserved sperm from a PR-M–expressing male and newly purchased Myh6-rtTA females. Progeny from these mice were used for microarray studies.

G. Genotyping

Genotyping was performed using PCR with DNA obtained from tail-snip tissue from mice aged 14 to 21 days. Bands were initially sequenced to verify authenticity. PCR bands were visualized on ethidium bromide–stained agarose gels.

H. Real-Time RT-PCR

Cardiac expression of PR-M was determined with SYBR Green (Life Science Research, Hercules, CA) real-time RT-PCR in all genotype-positive mice to determine expression levels. The control reaction consisted of mouse glyceraldehyde 3-phosphate dehydrogenase (mGAPDH) amplification. Reverse transcription was performed with a poly-T primer followed by PCR using a forward primer matching sequence in exon 1 of PR-M and a reverse primer complimentary to sequence in the fifth exon of PR-M. All reactions included three controls of reverse transcription without RNA, PCR without cDNA, and PCR without enzyme. Reactions showing an authentic melt curve in the negative controls were excluded. Expression level of PR-M was determined in cycles with authentic melt curves and evaluated by the formula: expression = [2 − (PR-M threshold cycle [Ct] − mGAPDH Ct)] × 100,000. Amplification efficiency was determined twice for mGAPDH and three times for PR-M using a cDNA concentration curve and found to be ~100% with <5% variance. Expression frequency analysis showed a bimodal distribution. Prior to data analysis, positive expression of PR-M was assigned to a value of >1.

SYBR Green (Life Sciences) real-time RT-PCR was also used to analyze gene expression of candidate genes with a more than twofold change identified in microarray studies and in the H9c2 cell line expressing PR-M treated with R5020. These included sarcolipin (Sln), myosin light polypeptide 4 (Myl4), fructose bisphosphate aldolase B (Aldob), natriuretic peptide type B (Nppb), and adenosine monophosphate deaminase 2 (AMPD2). Gene expression levels between PR-M–expressing and PR-M–nonexpressing mice were compared with the $\Delta\Delta$Ct method in which the nonexpressing mice were considered the reference group. In the H9c2 cells, an additional control included transfection to express an altered PR-M in which the initial 16 amino acids were deleted [8].

I. Metabolite Determination

Metabolomic analysis was performed using left ventricular apical tissue collected from seven male mice expressing PR-M treated with progesterone and eight male mice not expressing PR-M treated with progesterone for 4 weeks. Amino acids, free carnitine, acylcarnitines, and organic acids were analyzed using stable isotope dilution techniques. Amino acids and acylcarnitine measurements were made by flow injection tandem mass spectrometry using sample preparation methods described previously [12, 13]. The data were acquired using a Waters Acquity™ UPLC system equipped with a triple quadrupole detector and a data system controlled by MassLynx 4.1 operating system (Waters, Milford, MA). Organic acids were quantified using methods described previously employing Trace Ultra GC coupled to ISQ mass spectrometer operating under Xcalibur 2.2 (Thermo Fisher Scientific) [14].

J. Microarray

Total RNA (DNase I treated) was isolated from heart tissue of three male mice expressing PR-M (pos) and three male mice not expressing PR-M (neg). In each case, the same location of

ventricle (apical) was used. All three pos mice were littermates, whereas two of the neg mice were littermates, and the third neg mouse was from different parents. All mice were treated for 19 to 21 days with Dox-containing food and water. One week after the start of Dox, daily subcutaneous injections of 2.5 mg progesterone in ethyl oleate were administered for 12 to 14 days. Microarray analysis was performed after 3′ *in vitro* transcription using a GeneChip® Mouse Genome 430 2.0 Array (Affymetrix, Santa Clara, CA). Data normalization, analysis, hierarchical clustering, and gene ontology enrichment were performed with Partek Genomics Suite 6.6 software (Partek Inc., St. Louis, MO). Gene expression with a twofold change and $P \leq 0.05$ was identified. Gene characteristic profiling was performed with Database for Annotation, Visualization and Integrated Discovery Bioinformatics Resources 6.7 using genes with a >1.25 fold-change and a $P \leq 0.01$. A parameter was considered significant with a corrected $P \leq 0.05$ (Benjamin-Hochberg). Gene set enrichment analysis (GSEA) was performed using the array data within GenePattern software from the Broad Institute [15]. Enriched gene sets were identified from the hallmark gene set (h.all.v5.0.symbols) collapsing the probe level data to gene symbols based on maximum expression and using gene set permutation. Pathways were visualized using Cytoscape 3.0 with the WikiPathways plugin [16]. Data may be found in the Gene Expression Omnibus repository under accession number GSE108551.

K. cTAC Protocol

Female mice were ovariectomized at 5 to 6 weeks of age. All mice received Dox starting at 6 to 7 weeks of age. Initially, mice were given regular food with Dox-treated water. Due to a low number of expressing mice, this was subsequently changed to a combination of Dox-containing food and water. At 7 to 8 weeks of age, daily subcutaneous injections of 2.5 mg progesterone in ethyl oleate or an equal volume of oil alone were started. cTAC [17, 18] was performed at 8 to 9 weeks of age. Echocardiograms were performed at 7 to 8, 8 to 9, 10 to 11, and 12 to 13 weeks. At 12 to 17 weeks of age, the *trans*-stenosis pressure gradient was determined followed by euthanasia and organ harvesting. Mice with a *trans*-stenosis pressure gradient of >15 mm Hg were included in analysis.

L. Echocardiograms

Echocardiograms were performed by one investigator (L.M.), blinded to genotype and treatment, with a Vevo® 2100 (FUJIFILM VisualSonics, Toronto, Ontario, Canada) ultrasound machine. Measured values were recorded in millimeters and included left ventricular end-diastolic dimension (LVDd), left ventricular end-systolic dimension (LVDs), interventricular septum thickness, and posterior wall thickness. HR was determined as beats per minute. All measurements were made in triplicate. The following calculated values were determined: percent fractional shortening (%FS) and mean velocity of circumferential shortening corrected by HR (mVcfc).

M. Immunohistochemical Staining

Immunohistochemical (IHC) staining was performed to determine the expression of recombinant PR-M in mouse heart and the degree of fibrosis and vascular density after cTAC. All samples were paraffin-embedded 5-μm sections. For the former, tissue was reacted with both a polyclonal PR antibody directed to the HBD (C19; Santa Cruz Biotechnology, Dallas, TX) [19] using alkaline phosphatase detection and with a mitochondrial marker antibody (MTC02; Abcam, Cambridge, MA) [20], using peroxidase detection. Sections were also stained with hematoxylin (Thermo Fisher Scientific). For determination of fibrosis and vascular density, sections were stained with Masson trichrome stain for the former and biotinylated Griffonia simplicifolia lectin (Vector Laboratories, Burlingame, CA) with peroxidase detection for the latter. Staining was quantified by scanning and obtaining images with Aperio ScanScope Slide Scanner and Aperio ImageScope Viewer (Leica Microsystems,

Buffalo Grove, IL). Fibrosis was determined by pixel count actions in Photoshop CS5 (Adobe Systems, San Jose, CA), whereas vascular density was calculated with the Analyze Particle function on ImageJ (National Institutes of Health, Bethesda, MD).

N. Estradiol and Progesterone Assay

Serum estradiol and progesterone levels were determined with a solid-phase competitive enzyme immunoassay [Abcam, Cambridge, MA (E2); Endocrine Technologies, Newark, CA (P4)].

O. Statistics

Data not normally distributed were natural log transformed for statistical analysis. Multiple sample comparisons were performed with ANOVA with least significant difference *post hoc* testing. Two-sample comparisons of means were performed with *t* test. Echocardiographic parameters were evaluated with two-way ANOVA and Tukey-Kramer adjustment using Statistical Analysis System 9.3 (SAS Institute, Inc., Cary, NC). Percent change in echocardiographic parameters between groups was evaluated with one-way ANOVA with Bonferroni *post hoc* testing or *t* test using IBM SPSS version 22 (IBM, Armonk, NY). For microarray analysis, raw data were normalized using robust multiarray average. Multiway ANOVA and fold change were performed to select target genes that were differentially expressed. Top differentially expressed genes were selected with P value of 0.05 based on ANOVA test and fold change cutoff of 2. Hierarchical clustering was performed on differentially expressed genes based on average linkage with Pearson dissimilarity. Gene ontology enrichment analysis on the gene lists was performed with χ^2 tests and limited to functional groups with more than two genes. Metabolite data were analyzed by unpaired *t* test with an *a priori* value of $P < 0.05$ considered significant. Seahorse analysis data were compared with two-factor ANOVA of transfection and treatment using *post hoc* Tukey honest significant difference testing.

2. Results

A. PR-M Is Expressed in a Tet-On Mouse Model

Figure 1 shows the expression of human PR-M in the mouse model. Genotyping revealed three founders with incorporation of PR-M, of which one line was lost during breeding, one was shown to lack inducible expression of PR-M, and the remaining line was used for all experimentation. The top gel image in Fig. 1A shows a genotype-positive PR-M mouse using amplification of mouse genomic PR as a control. The bottom gels in Fig. 1A show examples of mice genotypes positive for both PR-M and rtTA after crossbreeding. Recombinant protein expression was shown in cardiomyocytes of PR-M–positive mice after Dox induction using IHC staining (red) with concomitant staining of mitochondria (brown). The mitochondrial striated staining pattern in longitudinal sections is identical to that in other publications [21, 22]. Not all cardiac cells expressed PR-M, which is typical with the TET-On system [23]. No PR-M staining was seen in PR-M–negative mice (Fig. 1B; Supplemental Fig. 1 [9]). SYBR Green (Life Sciences) real-time RT-PCR was used to determine transcript levels in the heart, as not all induced PR-M genotype-positive mice expressed transcript. Frequency analysis of transcript levels showed a bimodal distribution. Prior to data analysis, the decision was made to consider mice expressing PR-M to have an expression of >1 using the formula, expression = $[2 - {}^{(\text{PR-M Ct} - \text{mGAPDH Ct})}] \times 100{,}000$ (Fig. 1C). Melt curve analysis showed a single product (Supplemental Fig. 2 [9]).

PR-M transcript levels were found only in genotype-positive mice for both PR-M and rtTA. Even though the TET-On expression system uses Dox for induction, the system was found to be leaky with low expression seen in some mice not receiving Dox, which is commonly reported

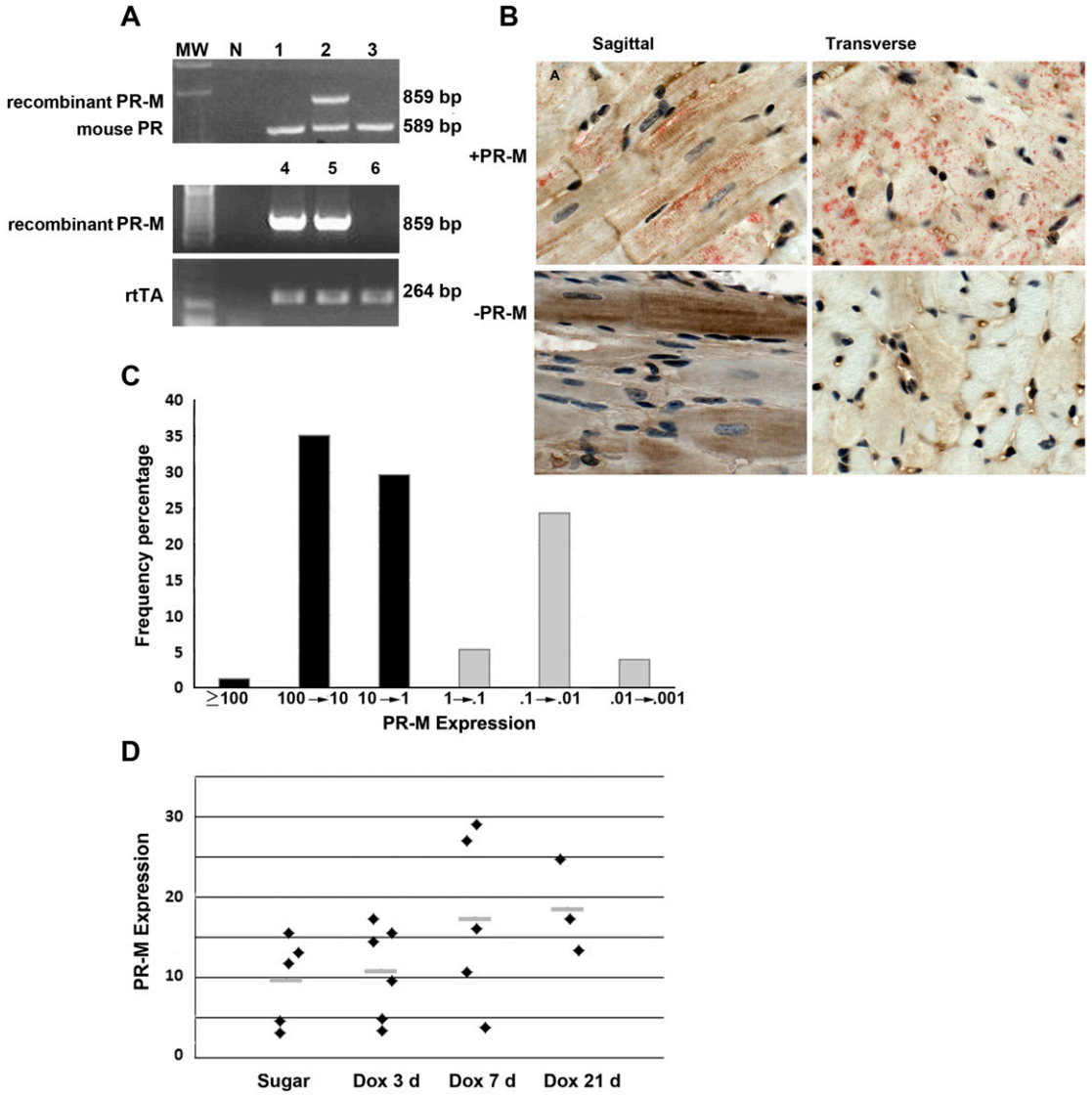

Figure 1. Expression of human PR-M. (A) Genotype results of PR-M–expressing mice prior to crossbreeding with rtTA mice (top). (B) IHC staining of cardiac tissue from a mouse expressing PR-M (+PR-M) and a mouse not expressing PR-M (−PR-M) showing red staining with the C19 PR antibody and brown with the mitochondrial protein antibody. (C) Cardiac PR-M expression as determined by SYBR Green real-time RT-PCR in all genotype double-positive mice. Positive expression was considered a value of >1. (D) Cardiac PR-M expression increased with exposure time to Dox, but the system was leaky with low levels of transcripts present without Dox exposure. No significant difference was seen among the four groups, but a significant difference was seen with pooling of the sugar and day 3 Dox compared with the pooled groups of day 7 and day 21 Dox groups ($P = 0.012$). Results are expressed as scatter plot with bar as mean. MW, molecular weight.

[24]. Expression with Dox treatment appeared to be maximum at 7 days (Fig. 1D). For this reason, all experimental mice received Dox, and expression was determined by real-time RT-PCR.

B. Cardiac Microarray Profile Shows Upregulation of Genes Associated With Sarcomere Development

Figure 2 shows microarray results from left apical ventricular tissue for male PR-M–expressing mice compared with PR-M–nonexpressing mice, both groups treated with progesterone (Fig. 2A). Principal component analysis showed considerable separation of the two groups (Fig.

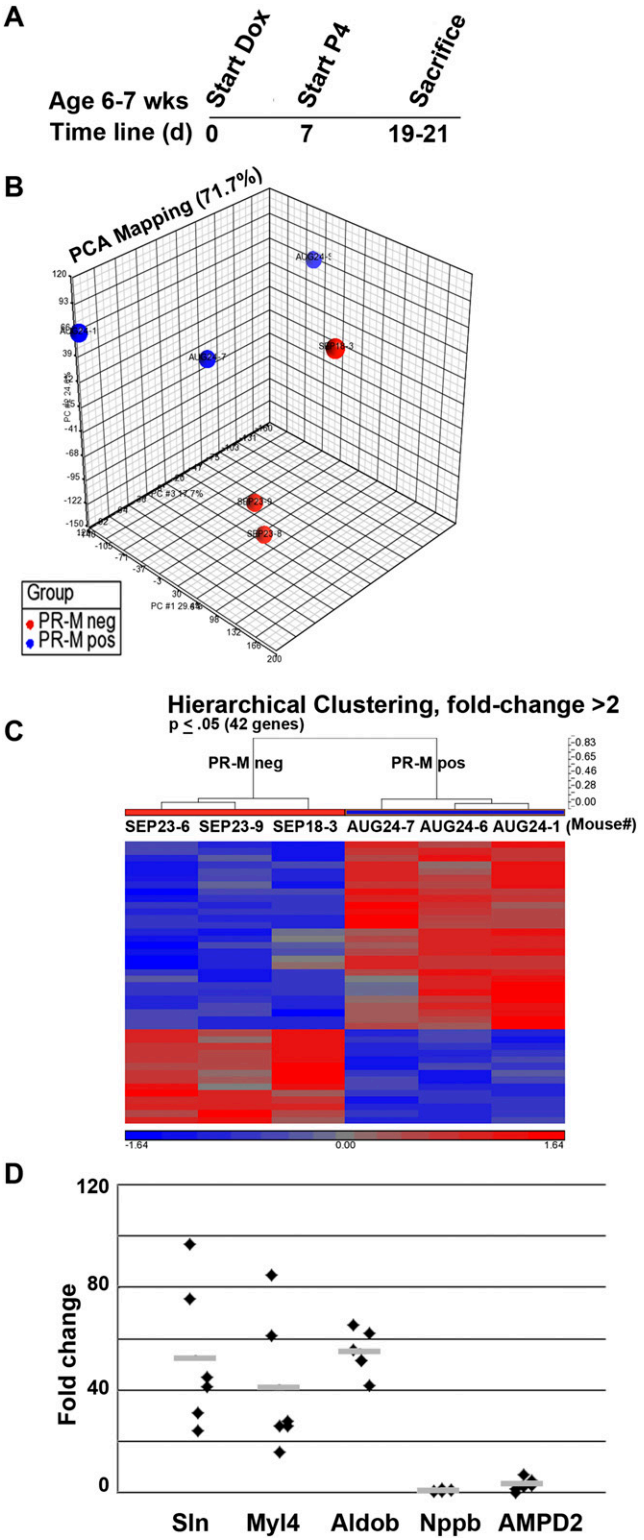

Figure 2. Microarray comparison of male mice expressing PR-M and mice not expressing PR-M treated with progesterone. (A) Shows the treatment protocol. (B) Shows separation of the two groups by principal component analysis (PCA). The hierarchical clustering heat map in (C) shows the majority of genes were upregulated in PR-M–expressing mice. (D) Expression of five genes (Mly4, Sln, Aldob, Nppb, and AMPD2) was verified with real-time RT-PCR. Only Ampd2 was discordant, showing a 2.4-fold downregulation on microarray but a 2.95-fold upregulation with real-time RT-PCR. Fold change values are mean ± SEM.

2B). In each group, mice were siblings, except for one mouse in the PR-M–nonexpressing group, possibly contributing to the variance in this group. Forty-two genes coding for 25 identified proteins showed a greater than twofold marked change between PR-M–expressing mice and PR-M–nonexpressing mice treated with progesterone. Of these, 17 were upregulated, whereas 8 were downregulated (Fig. 2C; Supplemental Table 1 [9]). The differences identified by microarray (Fig. 2D) were validated in five genes by real-time RT-PCR, including Myl4, Sln, fructose-bisphosphate Aldob, Nppb, and Ampd2. All genes were in agreement with the microarray except Ampd2. Whereas microarray showed a 2.3-fold downregulation, a 2.9-fold increase in transcript was identified by real-time RT-PCR. Database for Annotation, Visualization and Integrated Discovery bioinformatics analysis on 249 upregulated genes with >1.25-fold change ($P \leq 0.01$) showed ~50% to be phosphoproteins and 32% to be nuclear. No noteworthy parameters were found with 149 downregulated genes. In the total, 360 gene set keywords included phosphoprotein, alternative splicing, acetylation, and mRNA processing.

C. Cardiac Metabolomic and Microarray Profile Suggest Increased Cellular Energy Production in PR-M–Expressing Mice Treated With Progesterone

Targeted metabolic profiling was performed on apical ventricular samples from male mice that were expressing PR-M or not expressing PR-M and treated with progesterone for 4 weeks. Amino acids showed no significant changes between the genotypes (Supplemental Table 2 [9]), whereas the tricarboxylic acid (TCA) cycle metabolites succinate and malate trended lower (Fig. 3A; $P < 0.10$) in the PR-M–expressing mice but did not reach a significant difference. To gain insight into the status of cardiac fuel metabolism, levels of acylcarnitines were determined. Acylcarnitines are primarily mitochondrial-derived carnitine esters of acyl-CoA metabolites and thus reflect mitochondrial substrate selection [25]. A pattern emerged in the acylcarntines showing lower levels of many even-chain acylcarnitines (Fig. 3B), whereas the dietary-derived C16 and C18:1 acylcarnitines were unchanged (Fig. 3C). The lower acylcarnitines levels were also observed in several medium- and long-chain hydroxylated acylcarnitine species. These species are carnitine esters of the hydroxylated long-chain CoAs derived from enzymatic activity of the β-hydroxy-acyl CoA dehydrogenases in the third step of the mitochondrial beta-oxidation pathway (Fig. 3D and 3E). Importantly, tissue levels of free carnitine (C0) were unchanged, strongly suggesting that carnitine availability was not limiting the production of the acylcarnitine moieties in the PR-M–expressing mice (Supplemental Table 2 [9]). Because lower acylcarnitine content could reflect either higher or lower rates of fatty acid catabolism, energy-producing pathways from the GSEA were reviewed (Fig. 4A). These results revealed 19 gene sets showing enrichment with a false discovery rate <25% in PR-M–expressing mice. Myogenesis was a key upregulated pathway in response to progesterone action via PR-M. Interestingly, both the oxidative phosphorylation, containing many TCA cycle genes, and fatty acid metabolism gene sets showed significant enrichment (false discovery rate q value <0.06) in the PR-M–expressing mice (Fig. 4B and 4D). When gene expression data from the arrays were visualized using pathways for TCA cycle and beta-oxidation, it became evident that the expression of many key genes was elevated in the PR-M–expressing mice (Fig. 4C and 4E). For example, genes regulating fatty acid delivery [thrombospondin receptor (CD36) and carnitine palmitoyltransferase 1B], fatty acid activation (acyl-CoA synthetase long-chain family member), beta-oxidation (acyl-CoA dehydrogenase family member and Had), and acylcarnitine metabolism (carnitine palmitoyltransferase 2, Slc25a20, carnitine/acylcarnitine translocase, carnitine *O*-acetyltransferase, and carnitine *O*-octanoyltransferase) were overrepresented in the PR-M–expressing mice relative to PR-M–nonexpressing controls. In aggregate with the lower medium- and long-chain acylcarnitine production described previously, these data support the hypothesis that mitochondrial beta-oxidation may be enhanced by the expression of PR-M.

D. Rat Cardiomyocyte Cell Line (H9c2) Expressing PR-M Shows Ligand-Dependent Increase in Oxidative Cellular Respiration and Fatty Acid Oxidation

H9c2 cells expressing PR-M (Supplemental Fig. 3 [9]) showed a ligand-dependent substantial increase in gene expression of Myl4 and Sln, with a decrease in Nppb and Ampd2, similar to

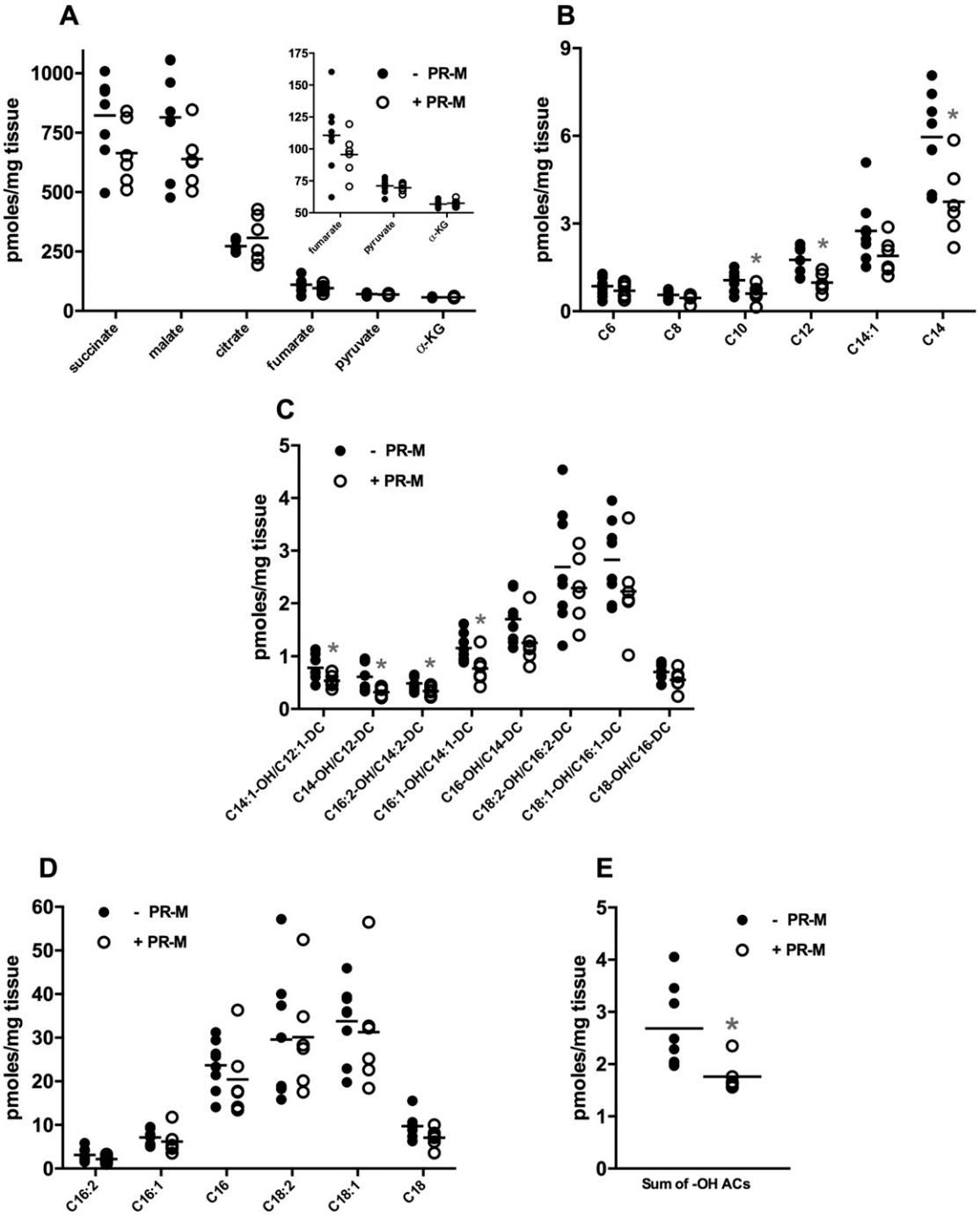

Figure 3. PR-M–expressing mouse hearts show diminished levels of medium- and hydroxylated long-chain acylcarnitines. Targeted metabolic profiling was conducted on flash-frozen ventricular tissue harvested from male mice. (A) Organic acids, (B) medium-chain acylcarnitines, (C) long-chain acylcarnitines, (D) hydroxylated acylcarnitines, and (E) sum of -OH acylcarnitines (ACs) chain length C8–C14. Results are expressed as scatter plot with bar as mean. N = 6–8 mice/genotype. *$P < 0.05$ vs PR-M–nonexpressing mice. α-KG, α-ketoglutarate.

the pattern seen in mouse heart (Fig. 5A–5E). Quantification of mitochondrial DNA showed no evidence of increased mitochondriogenesis (Fig. 5F). H9c2 cells were also transfected to express an altered PR-M in which the initial 16 amino acids were deleted [PR-M(−16aa)] [8]. This deletion resulted in loss of effect on the above-described gene expression (Supplemental Fig. 4 [9]). Parameters of cellular respiration (basal OCR, ATP-linked respiration, maximal

A.

Rank	NAME	SIZE	ES	NES
1	HALLMARK_EPITHELIAL_MESENCHYMAL_TRANSITION	184	0.4860	2.3076
2	HALLMARK_OXIDATIVE_PHOSPHORYLATION	183	0.4552	2.1280
3	HALLMARK_ADIPOGENESIS	179	0.4416	2.0634
4	HALLMARK_MYOGENESIS	188	0.3423	1.6032
5	HALLMARK_COAGULATION	128	0.3613	1.5866
6	HALLMARK_UV_RESPONSE_DN	132	0.3359	1.5164
7	HALLMARK_ANGIOGENESIS	33	0.4437	1.5116
8	HALLMARK_FATTY_ACID_METABOLISM	139	0.3244	1.4748
9	HALLMARK_ESTROGEN_RESPONSE_LATE	183	0.3032	1.4442
10	HALLMARK_GLYCOLYSIS	171	0.3053	1.4242

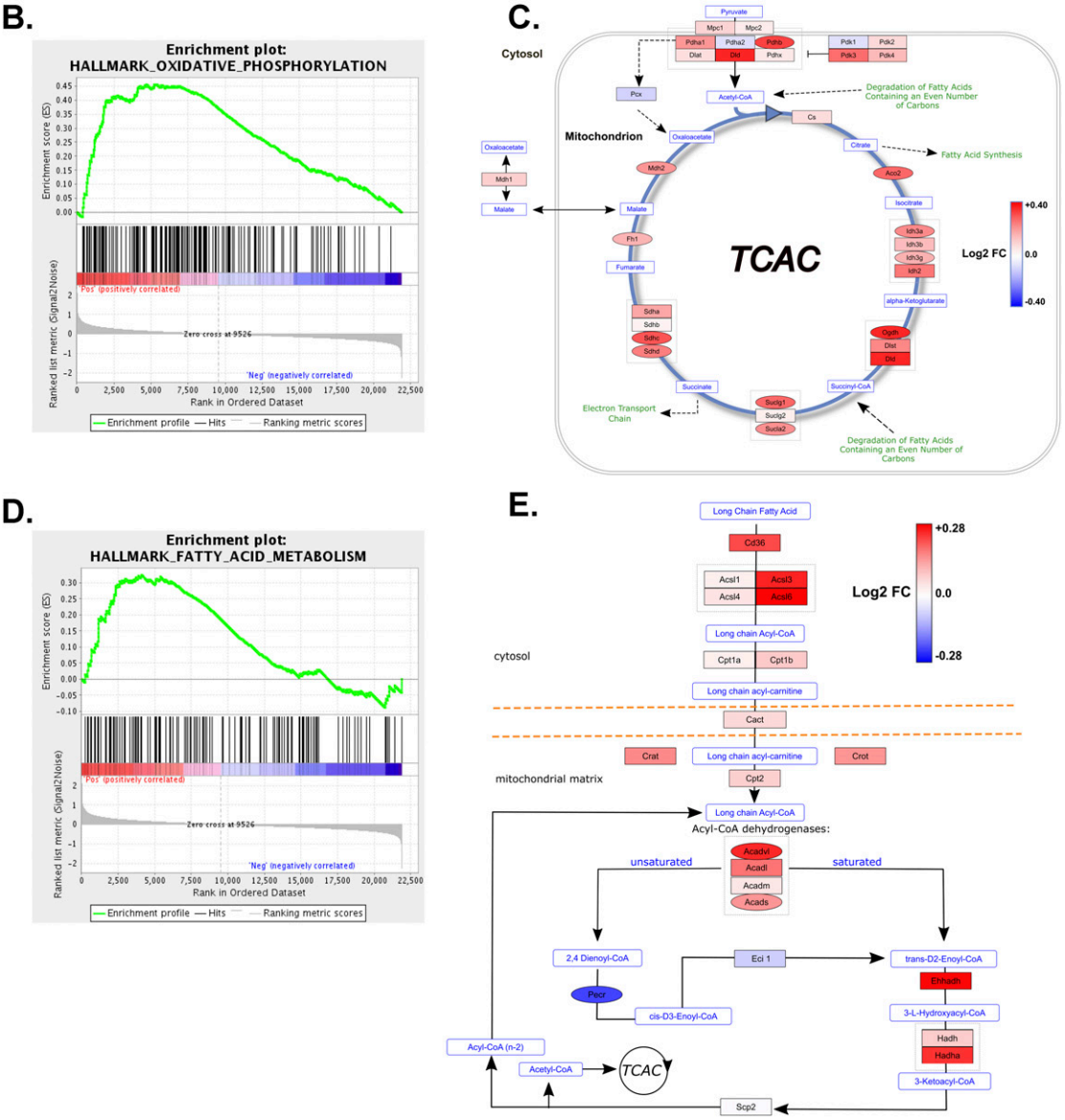

Figure 4. PR-M expression enriches for genes involved in mitochondrial metabolism. GSEA was performed using GenePattern software and Hallmark Gene Sets from the Molecular Signatures Database. (A) Top 10 enriched gene sets enriched in PR-M–expressing mice. (B and D) Enrichment plots of oxidative phosphorylation and fatty acid metabolism gene sets. (C and E) Pathway visualization of microarray expression data overlaid onto Wikipathways metabolic maps. Coloring of nodes represents log twofold change according to the scales in each figure. Shape of nodes represents uncorrected feature *P* values <0.05 (ovals) or >0.05 (rectangles).

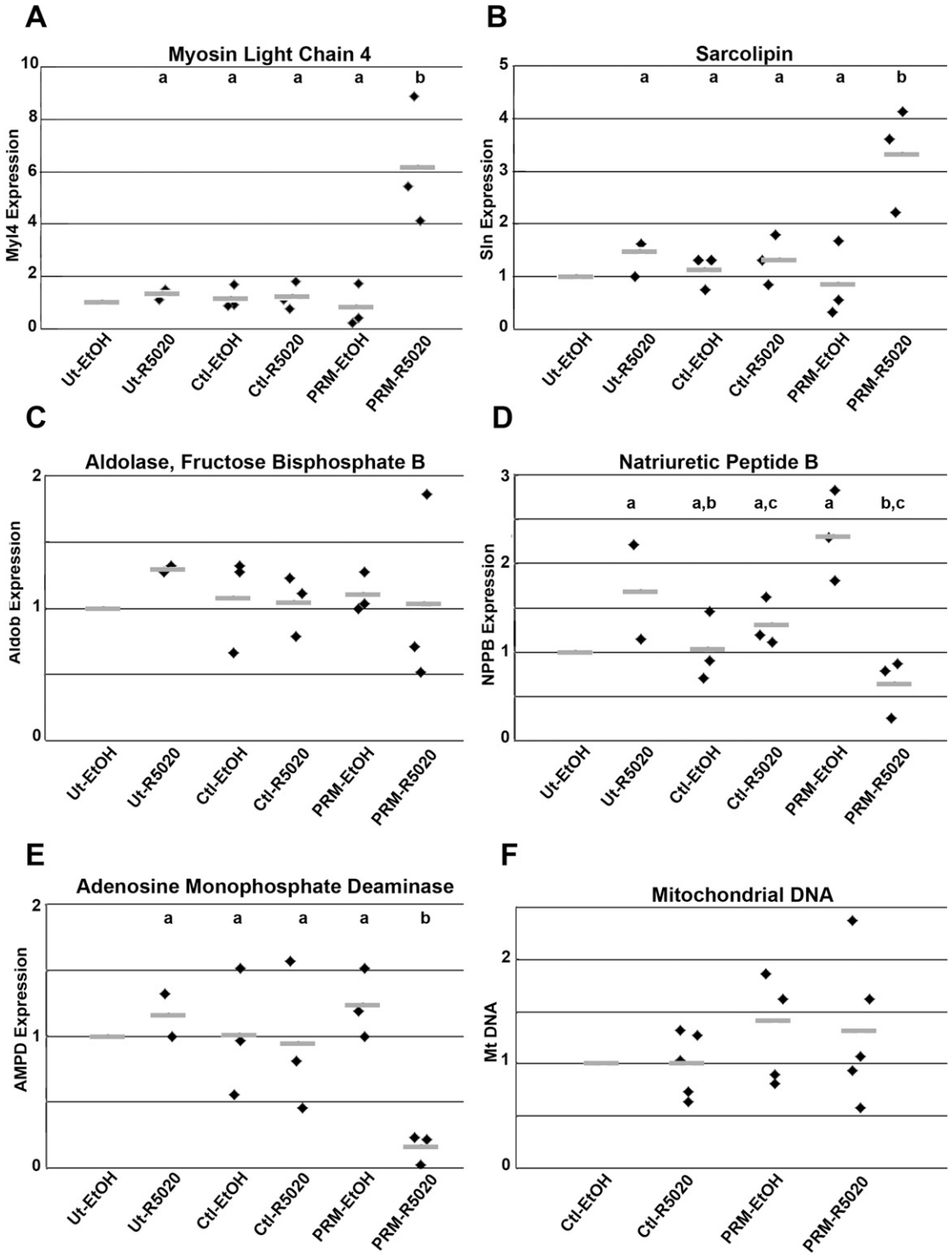

Figure 5. Mly4, Sln, Aldob, Nppb, and AMPD2 expression in H9c2 cells transfected with PR-M. Cells expressing PR-M treated with 10^{-6} M ligand R5020 (PRM-R5020) for 48 h showed increased expression of (A) Mly4 and (B) Sln compared with untransfected cells treated with R5020 (Ut-R5020), control plasmid–transfected cells treated with vehicle (Ctl-EtOH), control plasmid cells treated with R5020 (Ctl-R5020), and PRM-expressing plasmid treated with vehicle (PRM-EtOH). PRM-R5020 cells showed no difference in (C) Aldob expression, but decreased expression of (D) Nppb and (E) AMPD2. For $\Delta\Delta$Ct determination, rat GAPDH was used as the housekeeping gene and Ut-EtOH as the control condition. (F) With the same treatment, no change was seen in mitochondrial quantity as determined by

mitochondrial DNA (Mt DNA) using SYBR Green PCR. Nuclear DNA amplification was used as the reference and Ctl-EtOH as the control condition. Results are expressed in scatter plots with bar as mean. Treatments with different lettered superscripts are statistically different.

OCR, spare respiratory capacity, proton leak, and ECAR) were determined using the Seahorse XF^{e}24 Extracellular Flux Analyzer (Seahorse Bioscience). PR-M–expressing cells showed a ligand-dependent significant increase in basal OCR (P = 0.03; Fig. 6A) and ATP-linked OCR (P = 0.02; Fig. 6C), whereas maximal OCR (Fig. 6B) and spare capacity (Fig. 6D) approached a significant increase (P = 0.06). There was no increase in proton leak (Fig. 6E) or ECAR (reflecting glycolysis) (Supplemental Fig. 5 [9]). Increased fatty acid oxidation was shown with an increased production of ^3H_2O from tritium-labeled palmitate in cells expressing PR-M treated with ligand using a whole-cell assay (Fig. 6F).

E. Cardiac Expression of PR-M With Progesterone Treatment Decreases Heart Failure After cTAC

Given evidence of progesterone-mediated increases in cellular energy production and cardiac remodeling, we sought to determine an effect on cardiac stress. A model of heart failure induced by cTAC was chosen due to the rapidness and severity of echocardiographic changes observed with this model to increase the odds of determining an effect. Four groups of male mice, including mice expressing PR-M treated with progesterone or vehicle and mice not expressing PR-M treated with progesterone or vehicle, were analyzed. Two groups of ovariectomized female mice, including those expressing PR-M given progesterone and those not expressing PR-M given progesterone, were analyzed. The treatment schedule is shown in Fig. 7A. Blood progesterone levels (Fig. 7B and 7C) were supraphysiologic and similar in all progesterone-treated groups. Blood estradiol levels were not different between males and ovariectomized females (Supplemental Fig. 6 [9]). The *trans*-stenosis gradient (Fig. 7D and 7E) was greater in the male mice expressing PR-M treated with progesterone compared with PR-M–expressing male mice receiving vehicle and nonexpressing mice receiving vehicle (P = 0.003). There was no difference in the *trans*-stenosis gradient in female mice with or without PR-M expression. The PR-M expression level (Fig. 7F and 7G) was not significantly different in male mice receiving progesterone compared with mice receiving vehicle, whereas it was greater in male mice compared with female mice (P = 0.02). In general, there was no difference in echocardiographic parameters in the male or female groups before the initiation of progesterone compared with 1 week later on the day of the cTAC procedure (Supplemental Table 3 [9]). The exception being a greater LVDd in males not expressing PR-M treated with progesterone prior to initiation of progesterone compared with the day of cTAC (P = 0.034).

Figure 8 shows the percent change in male and female mice at 2 and 4 weeks after cTAC compared with before cTAC for parameters of LVDd, LVDs, and %FS. In males, the 4-week change in LVDs approached a significant difference (P = 0.071), with the greatest difference between the PR-M–expressing mice treated with progesterone and the PR-M–nonexpressing mice treated with progesterone (P = 0.056). A subset of male mice in these two groups were re-evaluated at 8 weeks, showing a more dramatic difference between PR-M–expressing mice treated with progesterone (n = 7 mice) compared with PR-M–nonexpressing mice treated with progesterone (n = 10) in LVDd (P = 0.042), LVDs (P = 0.007), and %FS (P = 0.008). No significant differences were seen between ovariectomized females expressing PR-M treated with progesterone and those not expressing PR-M treated with progesterone.

Supplemental Table 4 [9] shows the echocardiographic results in the groups of male and female mice at baseline (day of cTAC) and 2 weeks and 4 weeks after cTAC. Individual F statistics are shown in Supplemental Table 5 [9]. In male mice, there was a significant difference in all parameters with time within groups ($P < 0.01$). All male groups, except mice expressing PR-M treated with progesterone, showed increased left ventricular dimensions after cTAC. Contractility analysis showed worsening %FS and mVcFc in all groups except mice expressing PR-M treated

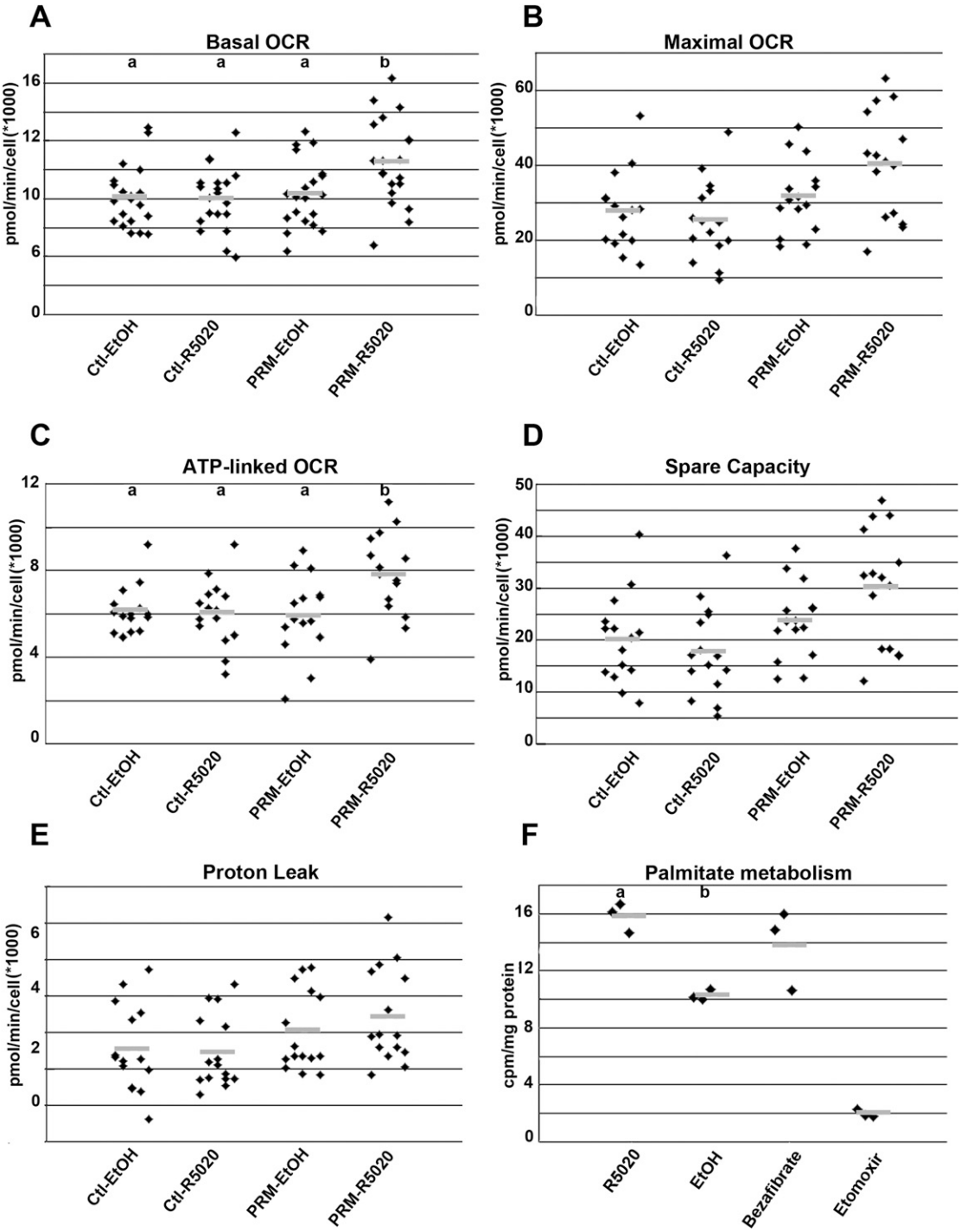

Figure 6. OCR and fatty acid oxidation in H9c2 cells expressing PR-M. Cells expressing PR-M treated with 10^{-6} M ligand R5020 (PRM-R5020) for 48 h showed increased (A) basal OCR and (C) ATP-linked OCR, whereas (B) maximum OCR and (D) spare capacity approached significance ($P = 0.06$). (E) There was no difference in proton leak. (F) With the same treatment, cells expressing PR-M showed increased oxidation of tritiated palmitate, with a positive control of bezafibrate and a negative control of etomoxir. Comparison treatments included control plasmid–transfected cells treated with vehicle (Ctl-EtOH), control plasmid cells treated with R5020 (Ctl-R5020), and PRM-expressing plasmid treated with vehicle (PRM-EtOH). Results are expressed in scatter plots with bar as mean. Treatments with different lettered superscripts are statistically different. cpm, counts per min.

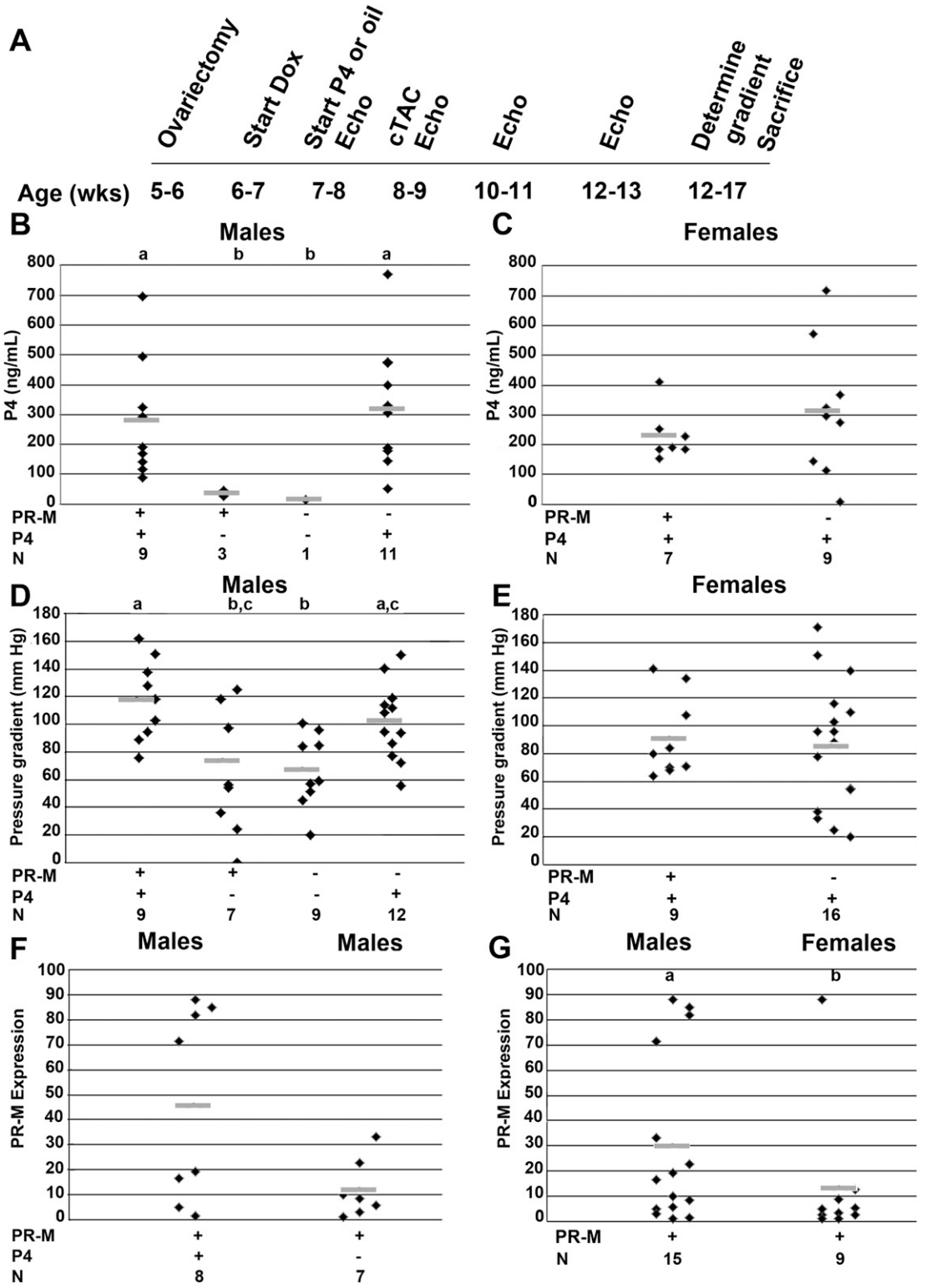

Figure 7. Study protocol for cTAC. (A) The timeline for male and female mice undergoing cTAC. (B and C) Blood progesterone levels in the treated male and female mice were supraphysiologic and not significantly different. (D and E) Transstenosis gradient was greater in the male mice expressing PR-M treated with progesterone compared with PR-M–expressing mice receiving vehicle ($P = 0.039$) and compared with nonexpressing mice receiving vehicle ($P = 0.007$). (F and G) PR-M expression levels were greater in male mice expressing PR-M treated with progesterone compared with male mice expressing PR-M

treated with vehicle. PR-M expression levels trended higher in males compared with females ($P = 0.07$). Groups with different lettered superscripts are significantly different. N represents the number of animals analyzed in each group. Results are expressed in scatter plots with bar as mean. Echo, echocardiogram.

with progesterone. An increase in septal wall and posterior wall thickness was in all groups. A significant difference in treatment between groups independent of time was seen for LVDd and LVDs ($P = 0.0057$ and $P = 0.02$), whereas a significant difference in treatment over time was seen with mVcfc ($P = 0.02$). Between-group comparisons at the same time point showed no difference at baseline. At 2 weeks and 4 weeks, mice expressing PR-M treated with progesterone had lower LVDd and LVDs compared with mice not expressing PR-M treated with progesterone. Mice not expressing PR-M treated with progesterone had greater ventricular dilatation compared with all groups. Regarding contractility, mice expressing PR-M treated with progesterone showed greater mVcFc at 4 weeks compared with mice not expressing PR-M treated with progesterone.

Female mice showed significant differences with time within groups for all parameters except LVDd ($P \leq 0.01$). Significant differences between baseline and 2 weeks and baseline and 4 weeks were seen with each parameter, except HR, in both PR-M–expressing mice and PR-M–nonexpressing mice treated with progesterone. Only female mice not expressing PR-M showed a significant decrease in HR.

F. Cardiac Expression of PR-M With Progesterone Treatment Decreases Cardiac Injury After cTAC

A subset of mice was studied for cardiac injury 8 weeks after cTAC. Evidence of cardiac protection in PR-M–expressing mice treated with progesterone was shown by increased capillary density ($P = 0.026$). A decrease in cardiac fibrosis in expressing mice compared with nonexpressing was not significant ($P = 0.27$; Supplemental Fig. 7 [9]). There was a significantly longer time from cTAC to euthanization (4 days) in the PR-M–expressing mice compared with the PR-M–nonexpressing mice ($P = 0.039$). We cannot exclude the possibility that these additional 4 days contributed to the histological findings.

G. GAPDH Levels Remain Consistent With PR-M Expression

Because GAPDH is an enzyme involved in glycolysis, consistency was evaluated to determine the possibility of change with PR-M expression, as this could potentially affect real-time RT-PCR results. There was no significant correlation of GAPDH Ct and PR-M Ct values ($r = 0.214$; $P = 0.3$). In the microarray studies, four probes were used to quantify GAPDH, and none showed a significant difference between mice expressing PR-M and those not (Supplemental Fig. 8 [9]). Likewise, there were no differences among the four male groups undergoing cTAC ($P = 0.7$) nor the two female groups ($P = 0.2$).

3. Discussion

Expression of the human PR-M in the mouse heart and H9c2 cells demonstrated a pattern of ligand-induced increase in oxidative cellular respiration with fatty acid metabolism and gene expression changes characteristic of remodeling and enhanced cellular metabolism. GSEA analysis of male mice expressing PR-M receiving progesterone compared with male mice not expressing PR-M receiving progesterone showed phenotypic enrichment of genes in both oxidative phosphorylation and fatty acid oxidation. This idea is supported by previous findings in which altered expression of PR-M, either by small interfering RNA knockdown in T47D breast cancer cells or overexpression in TET-ON HeLa cells, correlates with cellular respiration, as shown by change in mitochondrial membrane potential and cellular oxygen consumption [8].

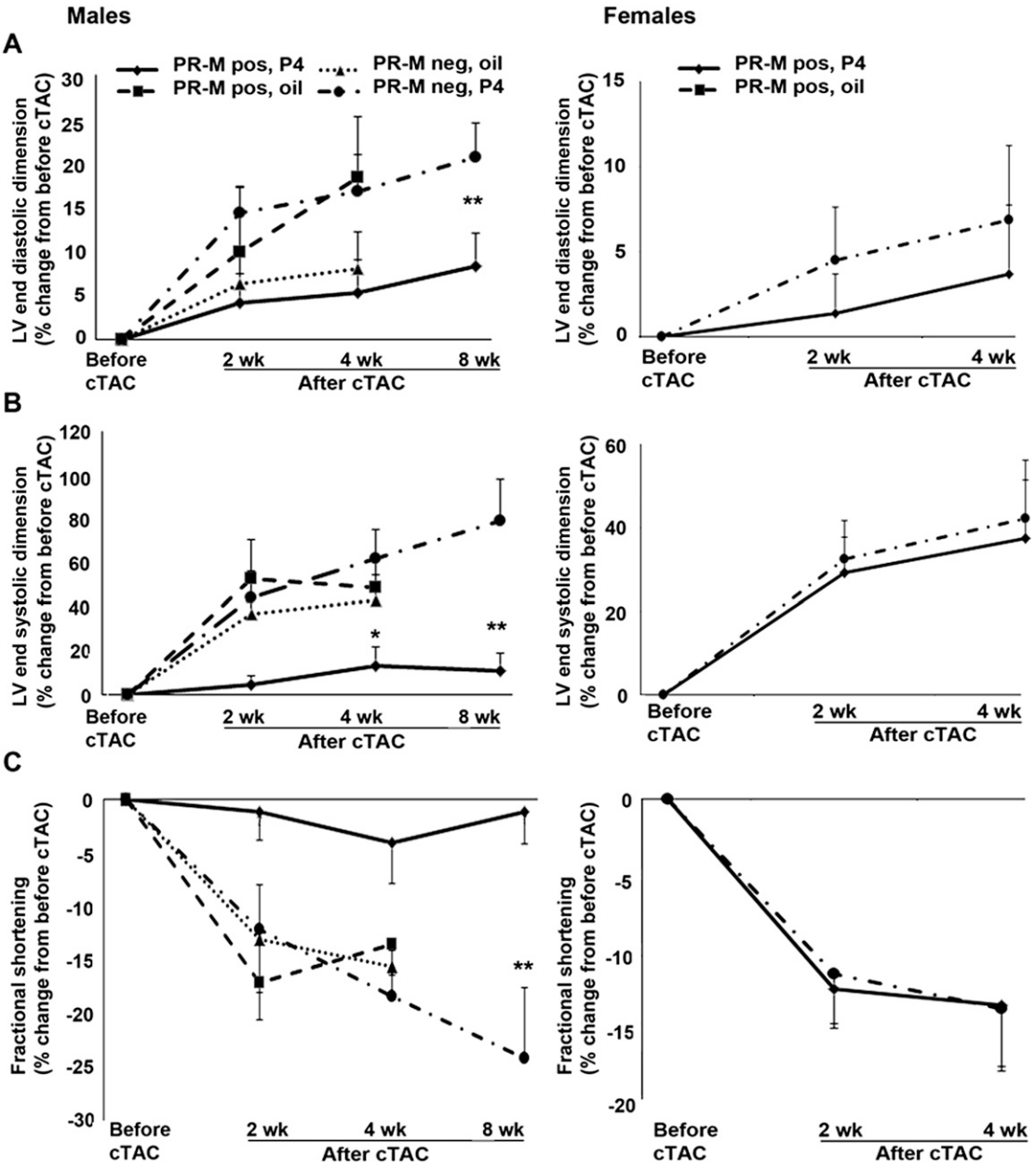

Figure 8. Percent change in echocardiographic parameters of (A) LVDd, (B) LVDs, and (C) %FS prior to and after cTAC. Male mice expressing PR-M treated with progesterone showed a lower LVDs at 4 wk after cTAC of borderline significance compared with nonexpressing mice treated with progesterone. A subset of male mice expressing PR-M treated with progesterone and nonexpressing mice treated with progesterone, observed at 8 wk after cTAC, showed more dramatic differences in parameters. No differences were seen in ovariectomized females expressing PR-M treated with progesterone compared with ovariectomized females not expressing PR-M treated with progesterone. Values are expressed as mean ± SEM. Number of mice are detailed in Supplemental Table 4 [9]. *P = 0.056; **LVDd, P = 0.042; LVDs, P = 0.007; and %FS, P = 0.008. LV, left ventricular.

Expression analysis showed overexpression of genes involved in sarcomere development, ATPase activity, and energy production. Cardiac muscle filament is composed of myosin molecules characterized by a hexamer of two heavy chains, each coupled with one essential light chain and one phosphorylated regulatory light chain. Myl4 encodes the essential light chain atrium (ELCa) protein normally expressed in the atrium, whereas Myl3 encodes the

ELC ventricle [26]. Ventricular expression of ELCa occurs in both exercise-induced PCH and pathological hypertrophic and dilated cardiomyopathies [27]. In comparison with ELC ventricle, ELCa complexed myosin shows faster kinetics, resulting in greater contraction force [28]. Thus, ELCa ventricular expression appears to be a compensatory mechanism to enhance function. A similar pattern was seen with the Myl7 gene encoding the atrial regulatory light chain.

Cardiac contractility is regulated by the ATP-dependent transport of calcium from the cytoplasm to the sarcoplasmic reticulum (SR) by the protein SR calcium ATPase (SERCA2a) encoded by ATP2a2. SERCA activity is regulated by the phosphoproteins phospholamban in the ventricle and Sln in the atrium. Under physiological conditions, phosphorylation leads to disassociation from SERCA, resulting in greater calcium transport into the SR, accelerating ventricular relaxation [29]. PR-M–expressing mice showed a 14.8-fold increase in Sln, a 1.3-fold increase in phospholamban ($P = 0.047$), and a 1.4-fold increase in SERCA2a ($P = 0.08$) compared with PR-M–nonexpressing mice.

The dramatic increase in Sln also suggests a compensatory uncoupling reaction in the ventricle. Muscle expression of Sln in rodents increases with high fat intake associated with increased fatty acid oxidation [30]. This protein uncouples calcium entry into the SR via SERCA, resulting in cellular thermogenesis [31]. This may be a key mechanism in diet-induced thermogenesis to prevent obesity in which fatty acids are consumed via heat production as opposed to being stored [32]. In our mouse model, it is possible that the increase in Sln is secondary to cardiac metabolic remodeling that seems to produce a signature of increased fatty acid uptake and utilization induced by progesterone via PR-M.

Nppb, also referred to as brain natriuretic peptide, was significantly downregulated in PR-M–expressing mice and rat cardiomyocytes. This protein is transcriptionally regulated in response to cardiomyocyte stretch and released from the ventricle to increase natriuresis and diuresis [33]. Interestingly, this downregulation was solely a hormonal response, as no surgery was performed on these mice, and their living conditions were identical to nonexpressing mice.

These findings suggest the production of progesterone initiates gene expression for cardiac remodeling independent of a volume change associated with pregnancy. Overall, the gene expression data suggest that progesterone via PR-M leads to protein synthesis required for sarcomere development and enhanced contractility even in the absence of hemodynamic changes resulting in myocardial stretch.

A functional effect was evaluated using a model of afterload-induced heart failure. This method of pathological hypertrophy was chosen instead of a model of physiological hypertrophy (swimming and running protocols) due to the more rapid and severe echocardiographic and histological changes [34]. Using echocardiogram parameters as markers for heart failure, the male group expressing PR-M treated with progesterone had the least change, whereas the mice not expressing PR-M treated with progesterone had the greatest. Activity of PR-M independent of ligand was unlikely given the better performance of the mice expressing PR-M treated with progesterone compared with those treated with vehicle. Likewise, there was no difference in the groups expressing PR-M and those not expressing PR-M treated with vehicle. Progesterone treatment in the absence of PR-M appeared detrimental, with this group having the most effect after cTAC. The lack of an endogenous PR-M gene in the mouse may contribute to this finding. Variables that could have affected the outcomes include differences in pressure gradient and PR-M expression levels. A greater pressure gradient in the mice expressing PR-M treated with progesterone compared with the mice expressing PR-M treated with vehicle makes the protective effect seen in the former group even more impressive given the greater workload on the heart. The detrimental effect of progesterone in control mice is supported by other studies. The addition of a progestin with estrogen exacerbated left ventricular remodeling after myocardial infarction with increased reactive oxygen species in a rat model [35], whereas *in vitro* application of progesterone to rabbit and guinea pig heart results in a negative inotropic effect [36, 37].

With females, two groups were compared, mice expressing PR-M treated with progesterone and mice not expressing PR-M treated with progesterone. There was no remarkable difference in cardiac parameters in females expressing PR-M with or without progesterone treatment. There are factors that may explain the difference between the male

and female mice. Males had a significantly higher PR-M expression compared with females that may have played a role in the sex discrepancy. Yet, sex differences in mouse cardiovascular experimentation are well recognized, with females having better function after induced myocardial infarction [38] and ischemic-reperfusion injury [39]. Intact female mice show less hypertrophic response after cTAC compared with males, with this difference being obviated by knockout of the estrogen receptor β (ERβ) receptor [40]. In addition, estrogen treatment of ovariectomized females decreases the hypertrophic response [41]. We found similar estradiol levels between male and ovariectomized females, suggesting the ovariectomy was properly performed and making it unlikely that endogenous estrogen levels would explain the sex difference. However, we did not evaluate ERα or ER$\alpha\beta$ levels, and the time frame of 1 week from ovariectomy to cTAC may have been inadequate to eliminate estrogen effects.

The transgenic human PR-M was recognized in mouse tissue by IHC staining using an antibody directed to the HBD of nPR as antibodies directed to the DNA-binding domain or the N-terminus would not recognize PR-M, given the structure, as shown in a previous publication [8]. Our staining showed no evidence of endogenous nPR expression in the mouse myocardium, which is supported by a previous study [42].

mGAPDH was used as the housekeeping gene control for real-time RT-PCR determination of PR-M expression. As this is a glycolytic enzyme, a change in the level could potentially increase pyruvate production, affecting oxidative phosphorylation. Also, increased mGAPDH would affect interpretation of PR-M expression. This did not seem to be the case, as mGAPDH Ct values showed no correlation with PR-M Ct values, there was no difference in levels with microarray analysis between PR-M–expressing and –nonexpressing mice, and there were no differences in the male and female groups undergoing cTAC. Additionally, previous research of rat neonatal heart cells cultured in glucose plus fatty acids compared with glucose alone showed no difference in GAPDH transcript levels [43].

There are limitations to our study. Findings in cardiac mouse models are not always applicable to human conditions given considerable differences including smaller size, 10 times higher HR, and 10 times shorter action potential [44]. The use of a heart failure model of cTAC is intended to model pathology secondary to aortic stenosis with relatively acute onset of failure. Using this model to study a potential mechanism applicable to pregnancy is not optimal, and other models of physiological hypertrophy, such as forced swimming or exercise, would be more representative of pregnancy-induced changes. There is also a selection bias with the cTAC model due to the high postprocedure mortality rate [45].

Another limitation is the expression of a protein not normally found in the mouse. There is no guarantee that the same downstream molecular pathways exist to represent the action of the transprotein. Yet there are examples in which this technique appears reliable. Expression of human *glutamate dehydrogenase 2* in the mouse results in the same protein localization [46], and the gene expression secondary to *glutamate dehydrogenase 2* expression mirrors that found in humans [47].

Our findings describe a fundamental process in which progesterone via a mitochondrial PR controls cellular energy production with an increase in fatty acid oxidation. In the heart, this pathway may explain the observation of increased fatty acid metabolism seen in reproductive-age women compared with men. This increased cardiac metabolism correlates with gene induction controlling energy production and remodeling to potentially meet the demands of pregnancy.

Acknowledgments

Mice were purchased from the Mutant Mouse Regional Resource Center and generated by the Duke Transgenic Mouse Facility. Metabolomics were performed by the Duke Sarah W. Stedman Nutrition and Metabolism Center at Duke University Medical Center. The Duke Microarray Core facility (an NCI Duke Cancer Institute and a Duke Genomic and Computational Biology shared resource facility) provided technical support, microarray data management, and feedback on the generation of the microarray data reported in this manuscript. Echocardiographic measurements were performed by the Duke Cardiovascular Research Center Animal Physiology Core Laboratory.

Financial Support: This work was supported by National Institutes of Health/National Institute of Child Health and Human Development Grant 5R03HD058017-02, the National Institutes of Health/National Institute of Environmental Health Sciences Grant T32ES021432, the Charles B. Hammond, MD, Research Fund, the Duke School of Medicine Voucher Program, and the Susan Fiery Hughes Memorial Research Foundation.

Correspondence: Thomas M. Price, MD, Division of Reproductive Endocrinology, Box 3928, Duke University Medical Center, Durham, North Carolina 27710. E-mail: price067@mc.duke.edu.

Disclosure Summary: The authors have nothing to disclose.

References and Notes

1. Ouzounian JG, Elkayam U. Physiologic changes during normal pregnancy and delivery. *Cardiol Clin*. 2012;**30**(3):317–329.
2. Foryst-Ludwig A, Kintscher U. Sex differences in exercise-induced cardiac hypertrophy. *Pflugers Arch*. 2013;**465**(5):731–737.
3. Melchiorre K, Sutherland GR, Liberati M, Thilaganathan B. Preeclampsia is associated with persistent postpartum cardiovascular impairment. *Hypertension*. 2011;**58**(4):709–715.
4. Demakis JG, Rahimtoola SH, Sutton GC, Meadows WR, Szanto PB, Tobin JR, Gunnar RM. Natural course of peripartum cardiomyopathy. *Circulation*. 1971;**44**(6):1053–1061.
5. Lopaschuk GD, Kelly DP. Signalling in cardiac metabolism. *Cardiovasc Res*. 2008;**79**(2):205–207.
6. Wittnich C, Tan L, Wallen J, Belanger M. Sex differences in myocardial metabolism and cardiac function: an emerging concept. *Pflugers Arch*. 2013;**465**(5):719–729.
7. Saner KJ, Welter BH, Zhang F, Hansen E, Dupont B, Wei Y, Price TM. Cloning and expression of a novel, truncated, progesterone receptor. *Mol Cell Endocrinol*. 2003;**200**(1-2):155–163.
8. Dai Q, Shah AA, Garde RV, Yonish BA, Zhang L, Medvitz NA, Miller SE, Hansen EL, Dunn CN, Price TM. A truncated progesterone receptor (PR-M) localizes to the mitochondrion and controls cellular respiration. *Mol Endocrinol*. 2013;**27**(5):741–753.
9. Dai Q, Likes CE III, Luz AL, Mao L, Yeh JS, Zhengzheng W, Kuchibhatla M, Ilkayeva OR, Koves TR, Price TM. Data from: A mitochondrial progesterone receptor increases cardiac beta-oxidation and remodeling. Dryad Digital Repository 2018. Deposited 14 December 2018. https://doi.org/10.5061/dryad.hb0338g.
10. RRID:CVCL_0286.
11. Manning NJ, Olpin SE, Pollitt RJ, Webley J. A comparison of [9,10-3H]palmitic and [9,10-3H]myristic acids for the detection of defects of fatty acid oxidation in intact cultured fibroblasts. *J Inherit Metab Dis*. 1990;**13**(1):58–68.
12. An J, Muoio DM, Shiota M, Fujimoto Y, Cline GW, Shulman GI, Koves TR, Stevens R, Millington D, Newgard CB. Hepatic expression of malonyl-CoA decarboxylase reverses muscle, liver and whole-animal insulin resistance. *Nat Med*. 2004;**10**(3):268–274.
13. Wu JY, Kao HJ, Li SC, Stevens R, Hillman S, Millington D, Chen YT. ENU mutagenesis identifies mice with mitochondrial branched-chain aminotransferase deficiency resembling human maple syrup urine disease. *J Clin Invest*. 2004;**113**(3):434–440.
14. Jensen MV, Joseph JW, Ilkayeva O, Burgess S, Lu D, Ronnebaum SM, Odegaard M, Becker TC, Sherry AD, Newgard CB. Compensatory responses to pyruvate carboxylase suppression in islet beta-cells. Preservation of glucose-stimulated insulin secretion. *J Biol Chem*. 2006;**281**(31):22342–22351.
15. Subramanian A, Tamayo P, Mootha VK, Mukherjee S, Ebert BL, Gillette MA, Paulovich A, Pomeroy SL, Golub TR, Lander ES, Mesirov JP. Gene set enrichment analysis: a knowledge-based approach for interpreting genome-wide expression profiles. *Proc Natl Acad Sci USA*. 2005;**102**(43):15545–15550.
16. Kutmon M, Lotia S, Evelo C, Pico A. WikiPathways App for Cytoscape: Making biological pathways amenable to network analysis and visualization [v2; ref status: indexed]. Vol. 3. *F1000Research*. 2014; **3**:152.
17. Esposito G, Rapacciuolo A, Naga Prasad SV, Takaoka H, Thomas SA, Koch WJ, Rockman HA. Genetic alterations that inhibit in vivo pressure-overload hypertrophy prevent cardiac dysfunction despite increased wall stress. *Circulation*. 2002;**105**(1):85–92.
18. Rockman HA, Ross RS, Harris AN, Knowlton KU, Steinhelper ME, Field LJ, Ross J Jr, Chien KR. Segregation of atrial-specific and inducible expression of an atrial natriuretic factor transgene in an in vivo murine model of cardiac hypertrophy. *Proc Natl Acad Sci USA*. 1991;**88**(18):8277–8281.
19. RRID:AB_632263.
20. RRID:AB_303683.

21. Andrienko T, Kuznetsov AV, Kaambre T, Usson Y, Orosco A, Appaix F, Tiivel T, Sikk P, Vendelin M, Margreiter R, Saks VA. Metabolic consequences of functional complexes of mitochondria, myofibrils and sarcoplasmic reticulum in muscle cells. *J Exp Biol*. 2003;**206**(Pt 12):2059–2072.
22. Kuznetsov AV, Margreiter R. Heterogeneity of mitochondria and mitochondrial function within cells as another level of mitochondrial complexity. *Int J Mol Sci*. 2009;**10**(4):1911–1929.
23. Takiguchi M, Dow LE, Prier JE, Carmichael CL, Kile BT, Turner SJ, Lowe SW, Huang DCS, Dickins RA. Variability of inducible expression across the hematopoietic system of tetracycline transactivator transgenic mice. *PLoS One*. 2013;**8**(1):e54009.
24. Zhu Z, Zheng T, Lee CG, Homer RJ, Elias JA. Tetracycline-controlled transcriptional regulation systems: advances and application in transgenic animal modeling. *Semin Cell Dev Biol*. 2002;**13**(2): 121–128.
25. Williamson J. Mitochondrial function in the heart. *Ann Rev Physiol*. 1979;**41**:485–506.
26. Hernandez OM, Jones M, Guzman G, Szczesna-Cordary D. Myosin essential light chain in health and disease. *Am J Physiol Heart Circ Physiol*. 2007;**292**(4):H1643–H1654.
27. Palmer BM. Thick filament proteins and performance in human heart failure. *Heart Fail Rev*. 2005; **10**(3):187–197.
28. Morano I, Hädicke K, Haase H, Böhm M, Erdmann E, Schaub MC. Changes in essential myosin light chain isoform expression provide a molecular basis for isometric force regulation in the failing human heart. *J Mol Cell Cardiol*. 1997;**29**(4):1177–1187.
29. Minamisawa S, Hoshijima M, Chu G, Ward CA, Frank K, Gu Y, Martone ME, Wang Y, Ross J Jr, Kranias EG, Giles WR, Chien KR. Chronic phospholamban-sarcoplasmic reticulum calcium ATPase interaction is the critical calcium cycling defect in dilated cardiomyopathy. *Cell*. 1999;**99**(3):313–322.
30. Bal NC, Maurya SK, Sopariwala DH, Sahoo SK, Gupta SC, Shaikh SA, Pant M, Rowland LA, Bombardier E, Goonasekera SA, Tupling AR, Molkentin JD, Periasamy M. Sarcolipin is a newly identified regulator of muscle-based thermogenesis in mammals [published correction appears in *Nat Med*. 2012;**18**(12):1857]. *Nat Med*. 2012;**18**(10):1575–1579.
31. Smith WS, Broadbridge R, East JM, Lee AG. Sarcolipin uncouples hydrolysis of ATP from accumulation of Ca2+ by the Ca2+-ATPase of skeletal-muscle sarcoplasmic reticulum. *Biochem J*. 2002;**361**(Pt 2):277–286.
32. Bombardier E, Smith IC, Gamu D, Fajardo VA, Vigna C, Sayer RA, Gupta SC, Bal NC, Periasamy M, Tupling AR. Sarcolipin trumps β-adrenergic receptor signaling as the favored mechanism for muscle-based diet-induced thermogenesis. *FASEB J*. 2013;**27**(9):3871–3878.
33. de Lemos JA, McGuire DK, Drazner MH. B-type natriuretic peptide in cardiovascular disease. *Lancet*. 2003;**362**(9380):316–322.
34. Perrino C, Naga Prasad SV, Mao L, Noma T, Yan Z, Kim H-S, Smithies O, Rockman HA. Intermittent pressure overload triggers hypertrophy-independent cardiac dysfunction and vascular rarefaction. *J Clin Invest*. 2006;**116**(6):1547–1560.
35. Arias-Loza PA, Hu K, Frantz S, Dienesch C, Bayer B, Wu R, Ertl G, Pelzer T. Medroxyprogesterone acetate aggravates oxidative stress and left ventricular dysfunction in rats with chronic myocardial infarction. *Toxicol Pathol*. 2011;**39**(5):867–878.
36. Mendoza J, De Mello WC. Influence of progesterone on membrane potential and peak tension of myocardial fibres. *Cardiovasc Res*. 1974;**8**(3):352–361.
37. Raddino R, Poli E, Pelà G, Manca C. Action of steroid sex hormones on the isolated rabbit heart. *Pharmacology*. 1989;**38**(3):185–190.
38. Cavasin MA, Tao Z, Menon S, Yang X-P. Gender differences in cardiac function during early remodeling after acute myocardial infarction in mice. *Life Sci*. 2004;**75**(18):2181–2192.
39. Cross HR, Lu L, Steenbergen C, Philipson KD, Murphy E. Overexpression of the cardiac Na^+/Ca^{2+} exchanger increases susceptibility to ischemia/reperfusion injury in male, but not female, transgenic mice. *Circ Res*. 1998;**83**(12):1215–1223.
40. Skavdahl M, Steenbergen C, Clark J, Myers P, Demianenko T, Mao L, Rockman HA, Korach KS, Murphy E. Estrogen receptor-beta mediates male-female differences in the development of pressure overload hypertrophy. *Am J Physiol Heart Circ Physiol*. 2005;**288**(2):H469–H476.
41. van Eickels M, Grohé C, Cleutjens JPM, Janssen BJ, Wellens HJJ, Doevendans PA. 17β-estradiol attenuates the development of pressure-overload hypertrophy. *Circulation*. 2001;**104**(12):1419–1423.
42. Hochner-Celnikier D, Marandici A, Iohan F, Monder C. Estrogen and progesterone receptors in the organs of prenatal cynomolgus monkey and laboratory mouse. *Biol Reprod*. 1986;**35**(3):633–640.
43. van der Lee KAJM, Vork MM, De Vries JE, Willemsen PHM, Glatz JFC, Reneman RS, Van der Vusse GJ, Van Bilsen M. Long-chain fatty acid-induced changes in gene expression in neonatal cardiac myocytes. *J Lipid Res*. 2000;**41**(1):41–47.

44. Berry JM, Naseem RH, Rothermel BA, Hill JA. Models of cardiac hypertrophy and transition to heart failure. *Drug Discov Today Dis Models*. 2007;**4**(4):197–206.
45. Breckenridge R. Heart failure and mouse models. *Dis Model Mech*. 2010;**3**(3-4):138–143.
46. Plaitakis A, Kotzamani D, Petraki Z, Delidaki M, Rinotas V, Zaganas I, Douni E, Sidiropoulou K, Spanaki C. Transgenic mice carrying GLUD2 as a tool for studying the expressional and the functional adaptation of this positive selected gene in human brain evolution [published online ahead of print 18 May 2018]. *Neurochem Res*. 2019;**44**(1):154–169.
47. Li Q, Guo S, Jiang X, Bryk J, Naumann R, Enard W, Tomita M, Sugimoto M, Khaitovich P, Pääbo S. Mice carrying a human *GLUD2* gene recapitulate aspects of human transcriptome and metabolome development. *Proc Natl Acad Sci USA*. 2016;**113**(19):5358–5363.